High resolution numerical modeling of mesoscale island wakes and sensitivity to static topographic relief data

C. G. Nunalee, Á. Horváth, and S. Basu

We thank the reviewer's for their time and insightful comments. In light of the input from the reviewers, we have revised our original manuscript and are confident that we have thoroughly addressed all of their individual comments. Of particular note, the revised manuscript incorporates a third global terrain dataset (i.e., GMTED2010) which helps to reinforce the results gleaned from our GTOPO-based and SRTM-based model comparison. Furthermore, in the revised manuscript GMTED2010 and SRTM were both remapped from their native 7.5s and 3s resolutions to 30s resolution prior to ingestion into the WRF model's preprocessing system. The remapping was done by the USGS interfaces used to download the data. These interfaces can be found at http://dds.cr.usgs.gov/srtm/version2_1/SRTM30 and http://earthexplorer.usgs.gov for SRTM and GMTED2010, respectively. Once the 30s SRTM and GMTED2010 data was downloaded (i.e., SRTM30 and GMTED30) we examined whether the differences in model results associated with each terrain dataset were explicitly due to source dataset resolution or instead differences at a deeper level. As is shown in the revised manuscript, the significant differences between the GTOPO30, SRTM30, and GMTED30-based simulations are found even when terrain remapping is invoked which indicates that the resolution of the dataset is not necessarily the root cause of the modeled flow field differences. Below we provide point-by-point responses to individual comments.

Reviewer #1

This paper is well written. i suggest it to be published after resolving these issues:
1. Why the orography datasets are so different for this island? It is due to resolution and why?

As discussed above, this is an important question to address and what our new results show is that the differences in the orography between the different datasets is not necessarily due to resolution. This was determined because even with the use of terrain remapping from high resolution to 30s resolution the differences still remained. Given that spatial resolution is not the differentiating factor between GTOPO, SRTM, are GMTED, it is likely that the differences are due to the methods in which the different datasets were compiled.

What would be the larger scale influence of the orography difference?

This manuscript has focused on the implications of the orography difference on the atmospheric mesoscale. To understand the implications of these difference on a synoptic or global-climactic scale one would need to perform numerical simulations at those respective scales. Unfortunately, such experimentation is beyond the scope of the current work.

It is a good suggestion for future model studies to consider which dataset to use, however, I suggest to emphasize in both abstract and conclusion about what specific aspect to consider, resolution?

We have added a sentence to the end of the conclusion which essentially states that modelers could evaluate the uncertainty of their simulations to terrain dataset by comparing the agreement of available terrain datasets for the area of interest prior to performing numerical simulations.

Reviewer #2

This manuscript is well-written and the reviewer is delighted to see studies of the sensitivity to orographic height (which is usually not published by modeling groups or left as a detail not considered worthy of publication). That said, the reviewer is concerned about the way in which the orographic datasets are interpolated to the target resolution. As explained below, it seems likely that the differences in GTOPO30 and STRM are due to resolution differences and not the datasets per se.

We agree with the reviewer that the interpolation method could potentially play an important role in this study. That being said, we have re-run all of our simulations using terrain remapping of SRTM and GMTED to 30 second resolution before ingesting it into the WRF model's preprocessing system. This remapping was done by the USGS's web interface which allowed us to download the data at 30s resolution directly. As is shown in our new results, very little difference is observed compared to the previous results which indicates that the simulated differences between SRTM/GMTED and GTOPO are not explicitly due to source data spatial resolution.

The orographic height generated from GTOPO30 and SRTM as shown in Figure 3 look like two completely different mountains. In particular, the "GTOPO30 mountain" does not even look like a smoothed version of the "SRTM mountain. While this could be due to plotting cross sections that are not averaged along the other dimension, it could also be due to the interpolation method. If that is the case it is not surprising that the two simulations are drastically different.

The new figure 3 illustrates terrain profiles of Gran Canaria after terrain remapping was applied. As can be seen, the significant differences between GTOPO30 and SRTM30/GMTED30 are still present yet the differences between SRTM30 and GMTED30 are marginal. As a side note, the terrain profiles shown in figure 3 are not dependent upon a plotting cross-section, instead they represent a southern (3D) view of the modeled island.

The authors state that they use the default interpolation method to map elevation data from GTOPO30(approx. 1km)/STRM(approx. 300m) to the model grid (1km). If interpolation and not remapping is used to map from a higher resolution grid to a lower resolution grid, one ends up effectively sampling the value closest to the target grid point in question instead of averaging source grid values over a control volume (as is done in remapping). If indeed linear interpolation is used to map STRM data to the model grid, such sampling is occurring which will inevitably lead to higher elevations than if remapping is used. This does not happen with GTOPO30 since it has approximately the same resolution as the model grid. The reviewer therefore speculates that the GTOPO and STRM differences are due to not using remapping. The authors are kindly asked to use remapping for the STRM mapping. If the authors show cross sections of the raw topographic data they will likely show that STRM has much higher elevations than GTOPO simply because it is higher resolution and therefore resolving the peaks better. In that case the authors should not attribute the differences to the orograhic source dataset per se but the resolution of the topographic data. In any case, the manuscript demonstrates that orography rougher than GTOPO is needed to accurately simulate flow downstream of the obstacle. This leads to questions about the smoothing procedure. There are several techniques (e.g. envelope orography) that attempt to raise peak heights without introducing spurious noise in the solutions. Maybe such techniques would render the GTOPO-based elevations rough enough for producing more accurate results. How and how much the orography is smoothed might be as important as the raw datasets. As mentioned above, the differences may be more due to differences in the resolution of the raw elevation dataset rather than which dataset is used (for this particular case). The above needs to be discussed in the manuscript. It would be very interesting if the authors would investigate different smoothing algorithms (such as envelope orography) if they are easily accessible/doable (from a software perspective).

As discussed above, the revised manuscript used high resolution terrain datasets remapped to 30s prior to ingesting it into the WRF model’s preprocessing system. The remapping was done by the USGS and downloaded directly at the 30s resolution.

Many models also include effects of under-resolved orography in the parameterizations. These usually use the standard deviation of the under-resolved orography. Are such parameterizations used here? This should also be mentioned in the manuscript since such parameterizations could also lead to significantly different simulation results.

In the results presented here, no parametrization for under-resolved orography has been invoked. Conventionally, such parameterizations are used primarily for larger-scale numerical simulations when grid scales are significantly larger than the terrain dataset resolution. Such parameterizations are frequently used to account for the effect of gravity wave drag at the synoptic and/or global scale. Nonetheless, the revised manuscript has included a mention of under-resolved topography parameterizations in the conclusion.

Manuscript prepared for Geosci. Model Dev. Discuss.
with version 2014/09/16 7.15 Copernicus papers of the LaTeX class copernicus.cls.
Date: 18 June 2015

High resolution numerical modeling of mesoscale island wakes and sensitivity to static topographic relief data

C. G. Nunalee[1], Á. Horváth[2], and S. Basu[1]

[1]Department of Marine, Earth, and Atmospheric Sciences, North Carolina State University, Raleigh, NC, USA
[2]Leibniz Institute for Tropospheric Research, Leipzig, Germany

Correspondence to: C. G. Nunalee (cgnunale@ncsu.edu)

Abstract

Recent decades have witnessed a drastic increase in the fidelity of numerical weather prediction (NWP) modeling. Currently, both research-grade and operational NWP models regularly perform simulations with horizontal grid spacings as fine as 1 km. This migration towards higher resolution potentially improves NWP model solutions by increasing the resolvability of mesoscale processes and reducing dependency on empirical physics parameterizations. However, at the same time, the accuracy of high-resolution simulations, particularly in the atmospheric boundary layer (ABL), are also sensitive to orographic forcing which can have significant variability on the same spatial scale as, or smaller than, NWP model grids. Despite this sensitivity, many high resolution atmospheric simulations do not consider uncertainty with respect to selection of static terrain height dataset. In this paper, we use the Weather Research and Forecasting (WRF) model to simulate realistic cases of lower tropospheric flow over and downstream of mountainous islands using both the default global 30 s United States Geographic Survey terrain height dataset (GTOPO30)~~and the 3s~~, the Shuttle Radar Topography Mission (SRTM)~~terrain height dataset.~~ , and the Global Multi-resolution Terrain Elevation Dataset (GMTED2010) terrain height datasets. While the differences between the SRTM-based and GMTED2010-based simulations are extremely small, the GTOPO30-based simulations differ significantly. Our results demonstrate cases where the differences between ~~GTOPO30-based and SRTM-based model terrain height~~ the source terrain datasets are significant enough to produce entirely different orographic wake mechanics, such as vortex shedding vs. no vortex shedding. These results are also compared to MODIS visible satellite imagery and ASCAT near-surface wind retrievals, and highlight the importance of considering uncertain static boundary conditions when running high-resolution mesoscale models.

1 Introduction

Massively-parallel computing platforms now enable regional-scale numerical weather prediction (NWP) models[1] to be easily integrated with fine-scale grid spacings, down to approximately 1 km horizontally. A valuable benefit of such high-resolution models is their capability to simulate orographically induced flow phenomena. Examples of such phenomena include gap-winds (Mass et al., 2014), lee-rotors (Ágústsson and Ólafsson, 2014), and wake vortices (Li et al., 2008). The accuracy of model simulations of orographic flows has been verified against a suite of observational data including, but not limited to, ground-based instruments e.g., lidar (Lesouëf et al., 2013), mesonets (Bieringer et al., 2013); satellite-based remote sensing instruments e.g., ~~SAR~~ synthetic aperture radar (SAR) (Miglietta et al., 2013); and airborne measurement platforms e.g., aircraft (Gioli et al., 2014), radiosonde (Nunalee and Basu, 2014). Despite the increased resolvability, and overall fidelity, offered by finer resolution models as it pertains to orographic flows, mesoscale NWP models are still constrained by multiple factors such as necessary physics parameterizations (Doyle et al., 2013; Draxl et al., 2014). The treatment of sub-grid scale (i.e., sub-mesoscale) processes such as turbulence, radiative transfer, moisture phase change, etc. collectively contributes to the uncertainty of model solutions (see Coiffier, 2011). At the same time, it has also been demonstrated that model uncertainty can be increased through the prescription of inaccurate, or unrepresentative, time-dependent atmospheric boundary conditions (Kumar et al., 2011; Pielke, 2013). In the past decade, advanced data assimilation techniques, coupled with improved remote sensing capabilities, have been shown to reduce simulation uncertainty (Ancell et al., 2011; Bieringer et al., 2013) and increase forecast skill (Pu et al., 2013). While great efforts have been expended to identify sources of NWP error with respect to model configuration (i.e., physics parameterizations) and dynamic (meteorological) boundary conditions, often overlooked is the sensitivity of model solutions to static boundary conditions, namely topographic relief.

---

[1] In the context of this article, NWP models refer to models that may run in forecast or hindcast modes.

Presently, ~~there exists~~ several global terrain height datasets exist which can be used by regional-scale NWP models. One of the most used surface relief datasets, named GTOPO30, was developed by the United States Geographic Survey and comprised through a synthesis of numerous international digital elevation models. GTOPO30 contains maximum spatial resolution of 30 arc seconds and is the default dataset for many community models such as the Weather Research and Forecasting (WRF) model. Aside from GTOPO30 data, other satellite-derived global terrain height datasets ~~also exist~~ are also available such as the Shuttle Radar Topography Mission (SRTM) (Farr et al., 2007), and the ~~Advanced Spaceborne Thermal Emission and Reflection Radiometer (ASTER)~~ Global Multi-resolution Terrain Elevation Data (GMTED2010) (GMTED, 2011). These datasets offer higher spatial resolutions globally of 3 arc seconds and ~~1 arc second~~7.5 arc seconds, respectively. The construction of surface terrain height grids in NWP models from source datasets ~~, such as~~ (e.g., GTOPO30~~or SRTM,~~ , SRTM, and GMTED2010) typically involves sub-grid scale averaging of the source data, grid-scale spatial interpolation during data ingestion, and/or preprocessing smoothing effects (e.g., see the WRF model Preprocessing System Documentation; NCAR, 2014). Although in many circumstances these activities are necessary, they can effectively result in under-resolved topographic relief. Under-resolved terrain height implies that the NWP model generated terrain height does not fully capture the relevant features of the natural topography described by the source data (Jiménez and Dudhia, 2012) and can result in terrain height discrepancies on the order of tens to hundreds of meters (Jiménez and Dudhia, 2013). Such discrepancies have been shown to result in significant error in simulated low-level wind fields (Rife and Davis, 2005; Jiménez et al., 2010; Santos-Alamillos et al., 2013). Aside from under-resolved terrain height in modeled grids, which is essentially an oversimplification of the source terrain height data, we show in this paper that uncertainty in source terrain height datasets themselves can be significant enough to result in fundamental differences in simulated orographic flow mechanics. This ~~result~~ finding illustrates that the sensitivity of NWP models can be more complex than 1st-order biases recently documented by Teixeira et al. (2014).

In this paper, we simulate two realistic cases of atmospheric flow past mountainous islands; for each case, we run ~~the~~ WRF model simulations using GTOPO30~~and SRTM~~, SRTM, and GMTED2010 source terrain height data while keeping all other model configurations identical. From the results, we comment on the fundamental differences in simulated atmospheric wake patterns associated with the ~~two~~ three terrain height fields. At the same time we compare the simulated flow features to those ~~expected from~~ observed in visible satellite imagery. Our results will demonstrate that selection of terrain height source data can, in some cases, be critical to successfully capturing the fundamental mechanics of mesoscale orographic wakes.

2 Case studies and modeling details

Two historical atmospheric events were considered in this paper, both corresponding to cases of flow past mountainous islands. Since the islands were far from any upstream surface heterogeneity, only the local terrain features associated with the islands ~~acted to perturb~~ perturbed the local winds and consequent cloud structures. For these events, the wind wake characteristics associated with each island were indicated by distinct cloud structures captured ~~by~~ in visible satellite imagery ~~provided by~~ from the Moderate Resolution Imaging Spectroradiometer (MODIS) instrument. The modeled wind wake patterns of the events were compared to one another and the differences were documented in the context of the inferred wake patterns shown in satellite imagery.

The first, and primary, case study involved the Spanish island of Gran Canaria (GC) off the west coast of Northern Africa on 30 April 2007. MODIS visible satellite imagery from this day (Fig. **??**~~a~~1 left panel) revealed a coherent pattern of dipole vortices (i.e., von Kármán vortices) being shed downstream of GC~~around 10:30UTC~~. GC has a diameter of approximately 50 km at sea level and has a peak elevation of 1948 m ~~m. s.l.~~ MSL. GC's SRTM-based topography is shown in Fig. ~~**??**~~ 1 (right panel) for reference.

The second case study presented here involves flow past several islands which collectively comprise the Lesser Antilles (LA) in the Eastern Caribbean. On 31 July 2013, MODIS visible satellite imagery of the Lesser Antilles region ~~(Fig. ??c)~~ illustrated distinct wakes behind all of the major islands of the LA ~~.~~ (Fig. 2 left panel). Contrary to the GC case which had a coherent vortex shedding wake regime, the LA case had weak wind wakes where the rotation behind each island was not strong enough to counter the background wind flow. Furthermore, the wakes were correlated with a reduction in cumulus cloudiness and darker sea surface color, a phenomenon investigated by Smith et al. (1997). The windward islands of the LA are generally lower than GC but are, nonetheless, ~~are~~ predominately mountainous with peak elevations near 1 km for each island (see Table 1).

The corresponding near-surface wind retrievals from ASCAT (Advanced Scatterometer) instrument (Vogelzang et al., 2011) on the MetOp-B (Meteorological Operational) satellite are shown in Fig. ~~??d).~~ 2 (right panel). The speed of the predominantly east-southeasterly winds decreased from an upstream value of 7.5-9.0 m s^{-1} to 4.5-7.0 m s^{-1} in the lee of the islands. The maximum speed reduction and the width/length of the wind wake were correlated with island peak elevation. The slower winds in the wake lead to a smoother sea surface and, thus, increased specular reflection and decreased diffuse reflection, while the opposite is true for the rougher sea surface areas experiencing faster winds outside the wake. Depending on the sun-satellite geometry, this difference between the relative strengths of specular vs. diffuse reflection can result in both dark and bright island wakes. When the island is farther away from the solar specular point, as in the LA case, the wake is darker than the surrounding rougher sea surface. Contrarily, when the island is close to the specular point, as in the GC case, the wake appears brighter than the surrounding ocean surface.

The numerical simulations performed in this study used the Weather Research and Forecasting (WRF) model version 3.6.1 which was initialized by ERA-Interim reanalysis data (physics configurations are shown in Table 2). The simulations used a nested four domain configuration centered on the islands of interest. Of note, a horizontal grid spacing of 1 km was chosen in the inner-most domain (d04) while the parent domains (d03–d01) used grid spacings of 3, 9, and 27 km, respectively. Additionally, in d04 the control simulations used GTOPO30 terrain height while the experimental simulations used terrain height data ~~interpolated from SRTM 3 arc second data .~~ remapped from SRTM and GMTED2010 to 30 arc seconds (i.e., SRTM30 and GMTED30, respectively). SRTM30 data were made available by $http://dds.cr.usgs.gov/srtm/version2_1/SRTM30$ and GMTED30 data were downloaded from $http://earthexplorer.usgs.gov$. Domains d01, d02, and d03 used 10 ~~, 5, and~~ min, 2 ~~minGTOPO30 terrain height , respectively~~min, and 30 sec GTOPO terrain height (respectively) with one-way feedback. All other modeling variables were held constant between the control simulations and experimental simulations. For ~~both the original GTOPO30 and SRTM~~ each of the three terrain height fields, the default smoothing and interpolation methods were selected. That is, 1 pass of the built-in WRF Preprocessing System (WPS) smoother-desmoother and 4 point averaging interpolation, respectively.

3 Gran Canaria case study

In this section, we analyze the atmospheric flow patterns downstream of GC as simulated by the WRF model with GTOPO30~~terrain and SRTM terrain~~ , SRTM30, and GMTED30 terrain fields. Before beginning the analysis, we compare the discrepancies between the ~~two~~ three terrain height data fields ~~.~~ in the left panels of Figure 3~~presents a~~ . Here a southern view of the model terrain height for GC as generated by GTOPO30~~and SRTM~~, SRTM30, and GMTED30 is shown. Notice that ~~aside from increased ruggedness in the SRTM-based terrain height , there is also a~~ compared to GTOPO30, the SRTM30-based and GMTED30-based terrain height profiles have not only increased ruggedness but also led to a significant increase in peak terrain height of GC island of nearly 1 km. ~~Additionally,~~ Furthermore, the differences between the SRTM30 and GMTED30 terrain profiles are largely insignificant. Fig. 3 also illustrates the upstream mean potential temperature cross-section in the lower troposphere on ~~the day of~~ 30 April 2007. Within the potential temperature cross-section, a well-mixed planetary boundary layer (PBL) can be identified by the nearly constant potential temperature in the lowest 800 m of the atmosphere. Above this layer, in the free atmosphere, a thermal capping inversion was present. Most importantly for the purposes of this paper, ~~is that~~ the increase in peak elevation of GC with the ~~SRTM~~ SRTM30 and GMTED30 data makes the modeled GC island penetrate into the stably stratified free atmosphere.

~~As~~ Given that the original GTOPO30-based elevation of GC was ~~predominately~~ predominantly within the well mixed PBL, the simulated flow around it was mostly 3 dimensional. That is, the impinging air parcels were able to rise and cross the crest of the island barrier and then descend on the lee slope without significant buoyant restriction. This effect ~~acted to produce~~ produced the unorganized wake pattern shown in the ~~lower-left~~ upper right panel of Fig. 3. Alternatively, with the ~~SRTM-based~~ SRTM30-based and GMTED30-based elevation, the increased topographic steepness along with the layer of stable stratification beneath the maximum height of the island caused much of the flow to split and pass around the lateral flanks of GC. This flow behavior generated coherent lee vortices (i.e., von Kámán vortices) which were shed downstream of the island, similar to what was observed ~~by the~~ in MODIS satellite imagery shown in Fig. ~~??~~1 (left panel).

In addition to invoking differences in the simulated wake pattern of GC, the ~~SRTM-based and~~ GTOPO30-based~~simulations also produced substantial variability to~~, SRTM30-based, and GMTED30-based simulations also exhibited substantial variability in the wind regime ~~on~~ very near to GC itself. In Fig. 4, an instantaneous streamwise wind speed cross section is presented for ~~both~~ all three simulations. Of particular note is the wind speed extrema (greater than 17 m s^{-1}) on the crest of GC in the GTOPO30-based simulation. This zone of high wind speed was a result of the Venturi effect caused by compression of the air column as it passed over the crest of the island. Alternatively, in the ~~SRTM-based simulation~~ SRTM30-based and GMTED30-based simulations this zone of strong wind speed was not ~~simulated~~ present due to the lack of significant air column compression over GC. Instead, the lateral flow around GC ~~produces~~ produced a zone of weak wind speed along the island centerline with respect to the flow direction.

4 Lesser Antilles case study

The second case study presented here deals with boundary layer flow impinging on the Eastern slopes of the Lesser Antilles (LA) island archipelago. As can be seen in Fig. ~~??~~2, the wake signatures from all of the major islands in this region persisted for up to approximately 300 km downstream. Contrary to the GC case, the wake patterns in the LA case did not contain strong enough vorticity to counter the ambient wind speed and therefore coherent wake vortices did not form. This type of wake pattern has been called a weak wake pattern by Smith et al. (1997), and forms in conditions of slower wind speed and lower island height in comparison ~~with~~ to the vortex shedding patterns ~~with~~ in the GC case.

In the ~~upper~~ left panels of Fig. 5, the regional topographic relief is shown for the GTOPO30-based simulation vs. the ~~SRTM-based simulation~~SRTM30 and GMTED30-based simulations. Of particular note is the fact that the island of Dominica, one of the more prominent of the islands in the LA in the ~~SRTM-based simulation~~SRTM30/GMTED30-based simulations, is represented as flat (1 m ~~m.s.l.~~MSL) in the ~~the~~ GTOPO30-based model elevation. At the same time, other neighboring islands (e.g., St. Vincent) appear relatively similar, despite them being slightly smaller in size in the GTOPO30-based ~~model.~~ simulation. Again as in the GC case, SRTM30 and GMTED30 terrain fields are very similar.

The differences in the depiction of Dominica's relief ~~in the two~~ between the three simulations manifested in substantial differences in regards to the simulated 6 h mean surface wind speeds. The ~~lower~~ right panels in Fig. 5 show the mean surface wind fields simulated by the ~~two~~ three model runs. Most notably, the weak wind wake associated with Dominica is nearly non-existent in the GTOPO30-based simulation while it extends hundreds of km in the ~~SRTM based simulation~~SRTM30-based and GMTED30-based simulations. In addition, the zone of enhanced wind speed associated with funneling between Dominica and its northern neighbor of Guadeloupe is increased in the ~~SRTM-based simulation~~SRTM30/GMTED30-based simulations. Lastly, the unique shapes of the individual island wakes showed signs of variability between the GTOPO30 and ~~SRTM~~ SRTM30/GMTED30 based simulations.

5 Conclusions

In this work, we have simulated two realistic cases of atmospheric flow past mountainous islands using the WRF model. For each case, we explored the sensitivity of the simulated wake patterns with respect to ~~two~~ three different terrain height source datasets (i.e., GTOPO30~~and SRTM~~, SRTM, and GMTED2010). Our results show cases where ~~the differences in modeled~~ differences in source terrain height corresponded to fundamental differences in simulated wake mechanics. For the GC case, the simulation which used GTOPO30 terrain height had a peak island elevation ~~which was~~ nearly 1 km lower than that in the ~~SRTM-based simulation. For this case~~SRTM30-based and GMTED30-based model terrain. Despite this difference the SRTM30 and GMTED30 terrain was very similar. That being said, the GTOPO30-based terrain did not reach the stably stratified thermal inversion above the planetary boundary layer while the ~~SRTM-based~~ SRTM30 and GMTED30 terrain extended hundreds of meters into the free atmosphere. This difference resulted in substantially less vertical vorticity downstream of GC island, along with an area of wind speed extrema on the crest of the island in the GTOPO30-based simulation. In other words, the ~~SRTM-based simulation~~ SRTM30-based and GMTED30-based simulations produced more significant lateral flow around the island and downstream von Kármán vortices, in agreement with MODIS visible satellite imagery, while the GTOPO30-based simulation facilitated anomalous Venturi-type wind speed-up on the crest of the island and incoherent downstream vortices.

For the LA case, the GTOPO30-based model terrain represented the island of Dominica to be essentially flat and near sea level (i.e., 1 m ~~m.s.l.~~MSL) and consequently resulted in no surface wind wake pattern. At the same time, the ~~SRTM-based simulation~~ SRTM30-based and GMTED30-based simulations were almost identical and resulted in a weak wind wake field which extended hundreds of km downstream of Dominica. The latter ~~was~~ two results were similar to what was ~~illustrated~~ observed in visible satellite imagery and scatterometer surface wind retrievals.

This work explored the value of using representative terrain height source data for high resolution mesoscale modeling activities. ~~Moreover, it was highlighted~~ The results presented here indicate that the differences in simulated flow features associated with different terrain datasets is not a consequence of the terrain source spatial resolution but instead arise due to fundamental differences in the datasets. This conclusion is supported by the fact that significant differences were found despite first remapping the higher resolution SRTM and GMTED datasets to 30s (equal to that of GTOPO30) prior to ingesting the data into the WRF model's preprocessing system. Moreover, this finding highlights the fact that considerable care should be taken ~~while~~ when selecting orographic relief input data ~~when~~ for simulating atmospheric flow over, around, and downstream of remote mountainous islands (e.g., Gran Canaria and Dominica). That being said, future studies should evaluate the ~~accuracy~~ uncertainty of global terrain datasets for other locations and their representativeness for mesoscale modeling. At a basic level, this can be done by comparing the similarity, or dissimilarity, of available terrain datasets for the area of interest prior to performing numerical simulations. Furthermore, the use of parameterization methods which incorporate higher-level terrain data (e.g., the standard deviation of terrain height within a grid cell) may be able to provide improved terrain representation in simulations of island wakes (see (Jiménez and Dudhia, 2012)).

Acknowledgements. The authors acknowledge computational and financial support received from the Renaissance Computing Institute in addition to financial support received from the Department of Defense AFOSR under award number (FA9550-12-1-0449). Any opinions, findings and conclusions or recommendations expressed in this material are those of the authors and do not necessarily reflect the views of the Department of Defense. The authors also thank Jur Vogelzang and Ad Stoffelen of the Royal Netherlands Meteorological Institute (KNMI) for providing the experimental 6.25-km ASCAT winds.

References

Abrams, M., Hook, S., and Ramachandran, B.: ASTER User Handbook Version 2, Tech. rep., NASA – Jet Propulsion Laboratory, 4800, 2002.

Ágústsson, H. and Ólafsson, H.: Simulations of observed lee waves and rotor turbulence, Mon. Weather Rev., 142, 832–849, 2014.

Ancell, B. C., Mass, C. F., and Hakim, G. J.: Evaluation of surface analyses and forecasts with a multiscale ensemble Kalman filter in regions of complex terrain, Mon. Weather Rev., 139, 2008–2024, 2011.

Bieringer, P. E., Ray, P. S., and Annunzio, A. J.: The effect of topographic variability on initial condition sensitivity of low-level wind forecasts. Part II: Experiments using real terrain and observations, Mon. Weather Rev., 141, 2156–2172, 2013.

Chen, F. and Dudhia, J.: Coupling an advanced land-surface/hydrology model with the Penn State/NCAR MM5 modeling system, Mon. Weather Rev., 129, 587–604, 2001.

Coiffier, J.: Fundamentals of Numerical Weather Prediction, Cambridge University Press, 2011.

Doyle, J. D., Epifanio, C. C., Persson, A., Reinecke, P. A., and Zängl, G.: Mesoscale modeling over complex terrain: numerical and predictability perspectives, in: Mountain Weather Research and Forecasting, Springer, 531–589, 2013.

Draxl, C., Hahmann, A. N., Peña, A., and Giebel, G.: Evaluating winds and vertical wind shear from Weather Research and Forecasting model forecasts using seven planetary boundary layer schemes, Wind Energy, 17, 39–55, 2014.

Dudhia, J.: Numerical study of convection observed during the winter monsoon experiment using a mesoscale two-dimensional model, J. Atmos. Sci., 46, 3077–3107, 1989.

Farr, T. G., Rosen, P. A., Caro, E., Crippen, R., Duren, R., Hensley, S., Kobrick, M., Paller, M., Rodriguez, E., Roth, L., Seal, D., Shaffer, S., Shimada, J., Umland, J., Werner, M., Oskin, M., Burbank, D., and Alsdorf D.: The shuttle radar topography mission, Rev. Geophys., 45, RG2004, doi:10.1029/2005RG000183, 2007.

Gioli, B., Gualtieri, G., Busillo, C., Calastrini, F., Gozzini, B., and Miglietta, F.: Aircraft wind measurements to assess a coupled WRF-CALMET mesoscale system, Meteorol. Appl., 21, 117–128, 2014.

Global multi-resolution terrain elevation data 2010 (GMTED2010): http://pubs.er.usgs.gov/publication/ofr20111073

Hong, S.-Y., Dudhia, J., and Chen, S.-H.: A revised approach to ice microphysical processes for the bulk parameterization of clouds and precipitation, Mon. Weather Rev., 132, 103–120, 2004.

Hong, S.-Y., Noh, Y., and Dudhia, J.: A new vertical diffusion package with an explicit treatment of entrainment processes, Mon. Weather Rev., 134.9, 2318–2341, 2006.

Janjić, Z. I.: The step-mountain ETA coordinate model: further developments of the convection, viscous sublayer, and turbulence closure schemes, Mon. Weather Rev., 122, 927–945, 1994.

Jiménez, P. A., Dudhia, J., González-Rouco, J. F., Navarro, J., Montávez, J. P., and García-Bustamante, E.: A revised scheme for the WRF surface layer formulation. Mon. Weather Rev., 140(3), 898–918, 2012.

Jiménez, P. A. and Dudhia, J.: Improving the representation of resolved and unresolved topographic effects on surface wind in the WRF model, J. Appl. Meteorol. Clim., 51, 300–316, 2012.

Jiménez, P. A. and Dudhia, J.: On the ability of the WRF model to reproduce the surface wind direction over complex terrain, J. Appl. Meteorol. Clim., 52, 1610–1617, 2013.

Jiménez, P. A., González-Rouco, J. F., García-Bustamante, E., Navarro, J., Montávez, J. P., de Arellano, J. V.-G., Dudhia, J., and Muñoz-Roldan, A.: Surface wind regionalization over complex terrain: evaluation and analysis of a high-resolution WRF simulation, J. Appl. Meteorol. Clim., 49, 268–287, 2010.

Kain, J.: The Kain–Fritsch convective parameterization: an update, J. Appl. Meteorol., 43, 170–181, 2004.

Kumar, A., Done, J., Dudhia, J., and Niyogi, D.: Simulations of Cyclone Sidr in the Bay of Bengal with a high-resolution model: sensitivity to large-scale boundary forcing, Meteorol. Atmos. Phys., 114, 123–137, 2011.

Lesouëf, D., Gheusi, F., Chazette, P., Delmas, R., and Sanak, J.: Low tropospheric layers over Reunion Island in lidar-derived observations and a high-resolution model, Bound.-Layer Meteorol., 149, 425–453, 2013.

Li, X., Zheng, W., Zou, C., and Pichel, W.: A SAR observation and numerical study on ocean surface imprints of atmospheric vortex streets, Sensors, 8, 3321–3334, 2008.

Mass, C. F., Warner, M. D., and Steed, R.: Strong westerly wind events in the Strait of Juan de Fuca, Weather Forecast., 29, 445–465, 2014.

Miglietta, M. M., Zecchetto, S., and De Biasio, F.: A comparison of WRF model simulations with SAR wind data in two case studies of orographic lee waves over the Eastern Mediterranean Sea, Atmos. Res., 120, 127–146, 2013.

Mlawer, E., Taubman, S., Brown, P., Iacono, M., and Clough, S.: Radiative transfer for inhomogeneous atmosphere: RRTM, a validated correlated-k model for the longwave, J. Geophys. Res., 102, 16663–16682, 1997.

Monin, A. and Obukhov, A.: Basic laws of turbulent mixing in the surface layer of the atmosphere, Contrib. Geophys. Inst. Acad. Sci. USSR, 151, 163–187, 1954.

NCAR: User's Guide for Advanced Research WRF Modeling System: CH3, The WRF Preprocessing System, available at: http://www2.mmm.ucar.edu/wrf/users/docs/user_guide_V3/users_guide_chap3.htm (last access: 15 April 2014), 2014.

Nunalee, C. G. and Basu, S.: Mesoscale modeling of coastal low-level jets: implications for offshore wind resource estimation, Wind Energy, 17, 1199–1216, 2014.

~~Pielke Sr.~~

Pielke, R. A.: Mesoscale Meteorological Modeling, Vol. 98, Academic Press, Waltham, MA, USA Oxford, UK Amsterdam, the Netherlands, available at: http://books.google.com/books?hl=en&lr=&id=ExlFulltapcC&oi=fnd&pg=PR1&dq=mesoscale+meteorolo (last access: 17 March 2015), 2013.

Pu, Z., Zhang, H., and Anderson, J.: Ensemble Kalman filter assimilation of near-surface observations over complex terrain: comparison with 3DVAR for short-range forecasts, Tellus A, 65, 19620, doi:10.3402/tellusa.v65i0.19620, 2013.

Rife, D. L. and Davis, C. A.: Verification of temporal variations in mesoscale numerical wind forecasts, Mon. Weather Rev., 133, 3368–3381, 2005.

Santos-Alamillos, F., Pozo-Vázquez, D., Ruiz-Arias, J., Lara-Fanego, V., and Tovar-Pescador, J.: Analysis of WRF model wind estimate sensitivity to physics parameterization choice and terrain representation in Andalusia (Southern Spain), J. Appl. Meteorol. Clim., 52, 1592–1609, 2013.

Smith, R. B., Gleason, A. C., Gluhosky, P. A., and Grubišic, V.: The wake of St. Vincent, J. Atmos. Sci., 54, 606–623, 1997.

Teixeira, J. C., Carvalho, A. C., Carvalho, M. J., Luna, T., and Rocha, A.: Sensitivity of the WRF model to the lower boundary in an extreme precipitation event – Madeira island case study, Nat. Hazards Earth Syst. Sci., 14, 2009–2025, doi:10.5194/nhess-14-2009-2014, 2014.

Vogelzang, J., Stoffelen, A., Verhoef, A., and Figa-Saldaña, J.: On the quality of high-resolution scatterometer winds, J. Geophys. Res., 116, C10033, doi: 10.1029/2010JC006640, 2011.

Table 1. Peak elevations of the major islands in the Lesser Antilles arcepelago.

Symbol	**Island**	**Peak Elevation**
A	Guadeloupe	1467 m
B	Dominica	1447 m
C	Martinique	1397 m
D	St. Lucia	950 m
E	St. Vincent	1234 m
F	Grenada	840 m

Table 2. Model physics configurations.

Parameterization	Name	Referenc
Microphysics	WRF Single-Moment 5-class	Hong et a
Longwave Radiation	RRTM Longwave	Mlawer e
Shortwave Radiation	Dudhia Shortwave Radiation	Dudhia (
Convection	Kain–Fritsch (d01 and d02)	Kain (200
Land Surface	Noah Land Surface Model	Chen and
Planetary Boundary Layer	~~Mellor–Yamada–Janji~~Yonsei University	Hong et a
Surface Layer	~~Monin–Obukhov Similarity Theory~~ Revised MM5 Surface Layer	Jiménez

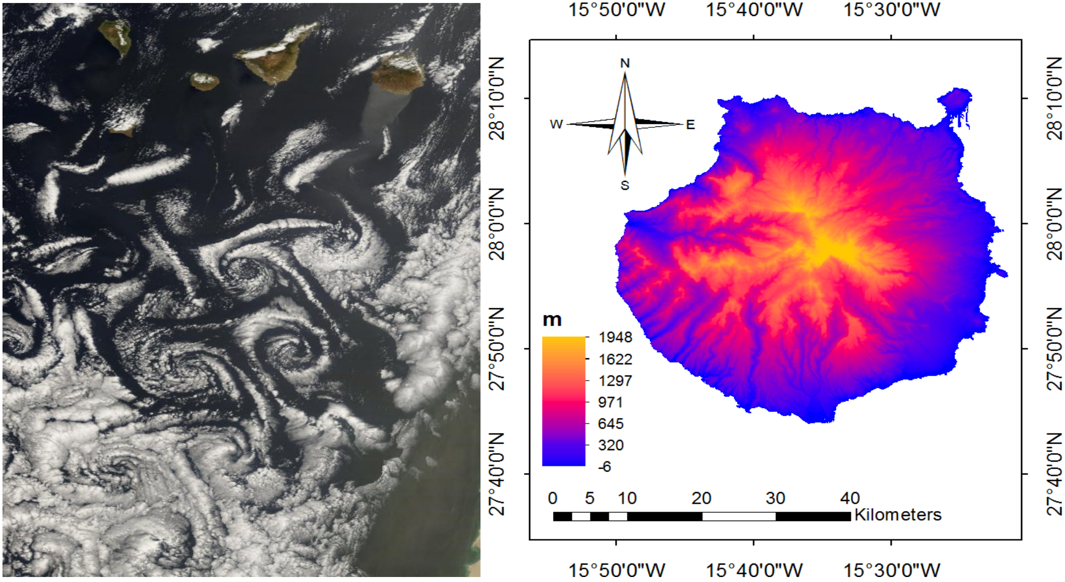

Figure 1. MODIS-TERRA visible satellite imagery of the Canary Islands on 30 April 2007 ~~with Gran Canaria in the upper~~ (left~~(a)~~) and SRTM terrain height profile of Gran Canaria ~~(b)~~(right).

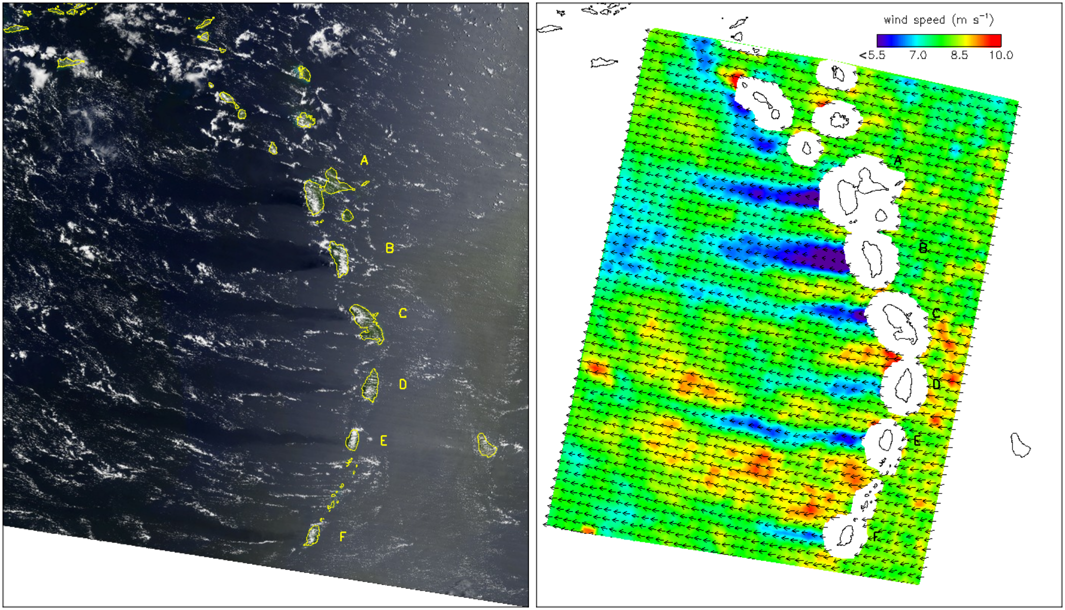

Figure 2. MODIS-TERRA true color image of the Lesser Antilles at 1440 UTC on 1 August 2013 (left panel). Note the dark island wakes embedded in sunglint in the eastern part of the image. Corresponding ASCAT-B 6.25-km resolution near-surface winds at 1326 UTC (right panel). For clarity, only every fourth wind vector is plotted.

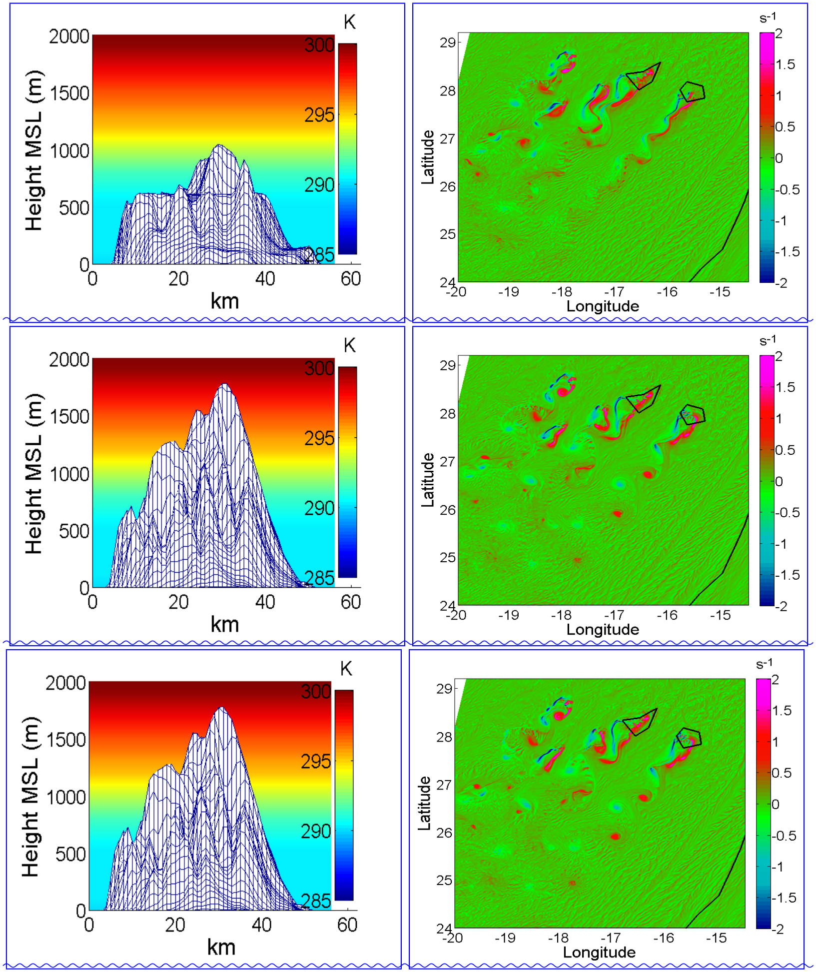
Height MSL (m)
2000
1500
1000
500
0
km
0
20
40
60
K
300
295
290
285
Latitude
29
28
27
26
25
24
Longitude
-20
-19
-18
-17
-16
-15
s-1
2
1.5
1
0.5
0
-0.5
-1
-1.5
-2

Figure 3. WRF model terrain height profiles of Gran Canaria as viewed from due South corresponding to GTOPO30 (upper left), SRTM30 (middle left), and GMTED30 (lower left). Background color-scheme represents ambient upstream potential temperature profile. Upper right, middle right, and lower right panels depict instantaneous relative vertical vorticity integrated vertically across the lowest 15 grid levels for the GTOPO30-based, SRTM30-based, and GMTED30-based simulations, respectively.

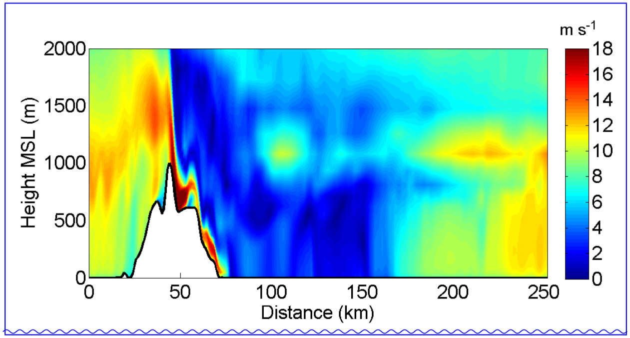
Height MSL (m)
2000
1500
1000
500
0
0
50
100
150
200
250
Distance (km)
m s-1
18
16
14
12
10
8
6
4
2
0

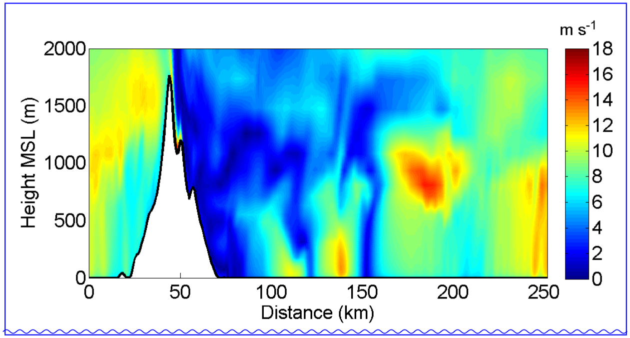
Height MSL (m)
2000
1500
1000
500
0
0
50
100
150
200
250
Distance (km)
m s-1
18
16
14
12
10
8
6
4
2
0

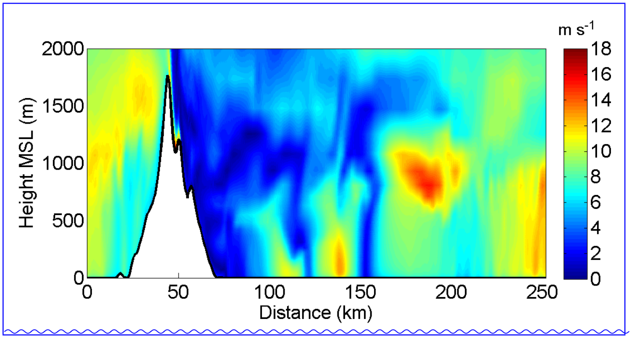
Height MSL (m)
2000
1500
1000
500
0
0
50
100
150
200
250
Distance (km)
m s-1
18
16
14
12
10
8
6
4
2
0

Figure 4. Instantaneous wind speed cross-sections for the GTOPO30-based (top panel), SRTM30-based (middle panel), and ~~SRTM-based~~ GMTED30-based (bottom panel) simulations at ~~10~~6:~~30~~00 UTC on 30 April 2007. Cross sections are oriented in the streamwise axis with inflow to the left.

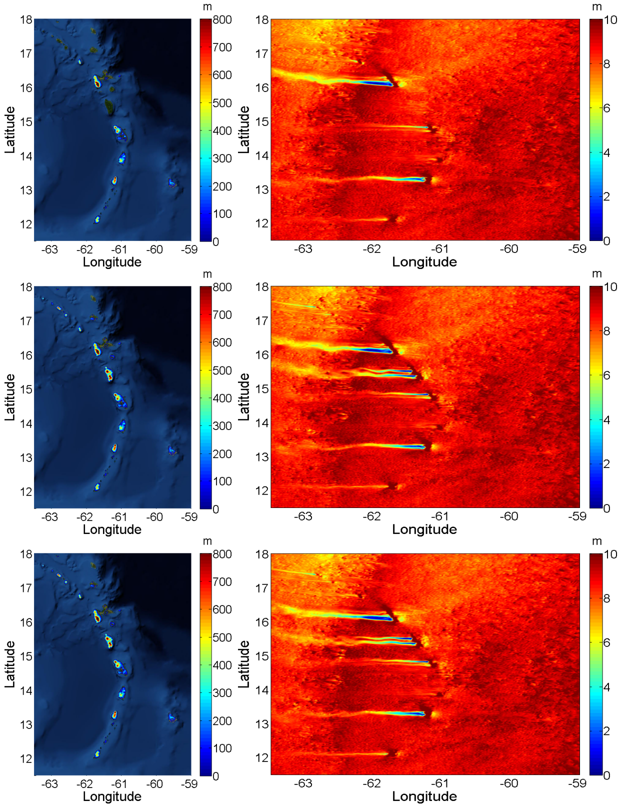

Figure 5. The WRF model's GTOPO30-based terrain height (upper left), SRTM30-based terrain height (middle left), and ~~interpolated SRTM~~ GMTED30-based terrain height (~~upper right~~lower left). ~~Lower left~~ Upper right, middle right, and lower right panels depict averaged wind speed in the boundary layer from 06:00–12:00 UTC as simulated by the GTOPO30-based~~run~~, SRTM30-based, and ~~SRTM-based run~~GMTED30-based runs, respectively.